



UNIVERSITÀ POLITECNICA DELLE MARCHE
Repository ISTITUZIONALE

Probabilistic seismic response assessment of linear systems equipped with nonlinear viscous dampers

This is the peer reviewed version of the following article:

Original

Probabilistic seismic response assessment of linear systems equipped with nonlinear viscous dampers / Tubaldi, Enrico; Ragni, Laura; Dall'Asta, Andrea. - In: EARTHQUAKE ENGINEERING & STRUCTURAL DYNAMICS. - ISSN 0098-8847. - STAMPA. - 44:1(2015), pp. 101-120. [10.1002/eqe.2461]

Availability:

This version is available at: 11566/225408 since: 2022-05-19T14:05:45Z

Publisher:

Published

DOI:10.1002/eqe.2461

Terms of use:

The terms and conditions for the reuse of this version of the manuscript are specified in the publishing policy. The use of copyrighted works requires the consent of the rights' holder (author or publisher). Works made available under a Creative Commons license or a Publisher's custom-made license can be used according to the terms and conditions contained therein. See editor's website for further information and terms and conditions.

This item was downloaded from IRIS Università Politecnica delle Marche (<https://iris.univpm.it>). When citing, please refer to the published version.

(Article begins on next page)

PROBABILISTIC SEISMIC RESPONSE ASSESSMENT OF LINEAR SYSTEMS EQUIPPED WITH NONLINEAR VISCOUS DAMPERS

E. Tubaldi¹, L. Ragni², A. Dall'Asta¹

¹School of Architecture and Design, University of Camerino, Viale della Rimembranza, 63100 Ascoli Piceno (AP), Italy; E-mail: etubaldi@gmail.com, andrea.dallasta@unicam.it

²Department of Civil and Building Engineering and Architecture, Polytechnic University of Marche, Via Breccie Bianche Ancona (AN), Italy; E-mail: laura.ragni@univpm.it

SUMMARY

The paper aims at evaluating the influence of damper properties on the probabilistic seismic response of structural systems equipped with nonlinear viscous dampers.

For this purpose, a linear single-degree-of-freedom system with an added linear or nonlinear viscous damper is considered, and the response statistics are evaluated for a set of natural records describing the ground motion uncertainty. A dimensional analysis of the seismic problem is carried out first to identify the minimum set of characteristic parameters describing the system and controlling the seismic response. An extensive parametric study is then carried out to estimate the influence of the damper properties on the statistics of the main response quantities of interest (i.e., maximum displacements, accelerations and damper forces), for a wide range of values of the characteristic parameters. Finally, a set of case studies is investigated in order to show some interesting issues concerning the influence of the damper nonlinear behaviour on the evaluation of the system reliability and to highlight some limitations of current deterministic approaches neglecting the probabilistic properties of the response.

KEYWORDS: nonlinear viscous dampers; probabilistic response; performance-based engineering; seismic risk.

INTRODUCTION

Supplemental energy dissipation systems are often used to enhance the performance of structures exposed to seismic hazard. In particular, viscous dampers provide an efficient tool to dissipate the seismic input energy into heat, by reducing both the displacement and force demand in the structures [1]-[3].

Experimental studies [4]-[6] have shown that the force-velocity relationship of viscous dampers can be analytically described by a velocity power law involving two parameters: the damping constant (c_N) and the velocity exponent (α), controlling respectively the damper's size and nonlinear behavior. Many works in the literature ([3],[7]-[13]) analyzed the steady-forced and earthquake response of frames equipped with linear or nonlinear viscous dampers by focusing on the sensitivity of the response to the damper exponent. In general, it was observed that nonlinear viscous dampers are more advantageous than linear dampers because they permit to achieve the same displacement reduction with lower forces in the damper. In all these above studies, which were mainly oriented to provide information useful for the damper design and the selection of the optimal damper properties, the seismic input was described by selecting a set of natural ground motions with different characteristics, and the seismic response was evaluated by averaging the results of the nonlinear time-history analyses for the different records. This approach is coherent with the prescriptions of several codes ([14]-[17]), which allow to consider only the mean values of the response parameters of interest for the performance assessment, provided that an adequate number of records is employed to describe the seismic input. However, this performance measurement, often referred to as "deterministic" [18], has a number of limitations since it does not account for the dispersion of

the response due to the input variability. Thus, it does not consider that systems with different properties (in particular with different velocity exponents α) may exhibit different sensitivities to the input variability and that certain response parameters may have higher dispersions than others. A more rigorous evaluation of the seismic performance of an engineered system should be carried out on a probabilistic basis and should aim at computing the effective statistical distribution of the various response parameters that affect the system reliability [18],[19]. This general statement is explicitly acknowledged in modern performance-based earthquake engineering (PBEE) frameworks such as the PEER framework [20][21] and the SAC-FEMA method [22], in latest seismic codes [23], and also in recent works on various structural damped systems [24]-[30].

In the technical literature, several studies developed within the context of stochastic dynamics [31]-[34] have employed analytical techniques to explicitly evaluate how the uncertainty in the seismic input (described by a stochastic model) propagates to the response in systems equipped with nonlinear viscous dampers. In this study, a different approach, consistent with the context of PBEE and latest seismic codes, is followed to evaluate the influence of the damper nonlinear behaviour on the seismic performance. In particular, the uncertainty in the seismic input is described by introducing a seismic intensity measure, and by considering a set of natural ground motions records characterized by a different duration and frequency content (which reflect the record-to-record variability) scaled to the same intensity measure. By this way, the statistics of the main response parameters of interest for the performance assessment can be estimated from the response samples obtained for the different ground motions.

The structural system considered in this paper consists of a single degree of freedom (SDOF) model coupling a linear visco-elastic term, representing the structural frame, and a linear or nonlinear purely viscous term, describing the added dissipative system. First, a nondimensionalization of the governing equation of seismic motion [35] is developed to find the minimum set of characteristic parameters that control the problem. Successively, a parametric study is carried out by varying these characteristic parameters within a range of interest for the design. For each combination of the characteristic parameters' values, the statistic of the response parameters of interest for the performance assessment (such as displacements, accelerations, and damper forces) is built based on the response samples. The influence of the damper nonlinear behavior and dissipation capacity on the probabilistic response is evaluated by observing the changes of the geometric mean and dispersion of the response parameters obtained with respect to a reference situation corresponding to the case of the system with no added dampers. Finally, the parametric study results are used to investigate the seismic performance, in terms of both probabilistic response and seismic risk, of a family of case studies consisting of the same structural system equipped with dampers having different properties (i.e., different values of c_N and α) ensuring the same deterministic performance objective. By this way, it is possible to evaluate the effect of the damper nonlinearity on the safety of the system and of its components.

It is noteworthy that although a simplified model has been considered in this study, the obtained results are relevant to the behaviour of more complex multi-degree of freedom systems equipped with damping devices, and shed light on potential drawbacks of current deterministic approaches employed in seismic codes and neglecting the probabilistic properties of the response.

NON DIMENSIONAL FORMULATION AND CHARACTERISTIC PARAMETERS

The equation of motion governing the seismic response of a single-degree-of-freedom (SDOF) system equipped with a nonlinear viscous damper can be expressed as:

$$m\ddot{u}(t) + c_L\dot{u}(t) + c_N|\dot{u}(t)|^\alpha \operatorname{sgn}(\dot{u}(t)) + ku(t) = -m\ddot{u}_g(t) \quad (1)$$

where $u(t)$ is the relative displacement of the mass to the ground, m , k , and c_L denote respectively the system mass, stiffness, and viscous (inherent) damping constant, c_N is the damping constant of the added non linear viscous damper, $\operatorname{sgn}(\cdot)$ is the sign function, $\ddot{u}_g(t)$ the ground motion input and

the dot denotes differentiation over time. The differential problem is completed by the initial conditions, assumed homogeneous in the following.

In order to reduce the equation to its non-dimensional form, the following dimensionless variables are introduced:

$$\begin{aligned}\psi &= u / u_0 \\ \tau &= t / t_0\end{aligned}\tag{2a,b}$$

where u_0 and t_0 are characteristic units measuring respectively the length and the time.

The seismic input can be expressed in terms of the product of a constant scale factor a_0 , whose dimension is an acceleration, and of a non-dimensional function $l(t)$, describing its variation over time:

$$\ddot{u}_g(t) = a_0 l(t) = a_0 \lambda(\tau)\tag{3}$$

where $\lambda(\tau)$ is obtained from $l(t)$ by scaling the time t by the factor $1/t_0$, according to Eqn.(2a). After substituting Eqns. (2a) and (3) into Eqn.(1) and rearranging, one obtains:

$$\ddot{\psi}(\tau) + \frac{c_L t_0}{m} \dot{\psi}(\tau) + \frac{c_N t_0^{2-\alpha}}{m u_0^{1-\alpha}} \text{sgn}(\dot{\psi}(\tau)) |\dot{\psi}(\tau)|^\alpha + \frac{k t_0^2}{m} \psi(\tau) = -\frac{t_0^2}{u_0} a_0 \lambda(\tau)\tag{4}$$

Finally, by choosing the time scale $t_0 = 1/\omega_0$, where $\omega_0 = \sqrt{k/m}$ denotes the system undamped circular frequency, and the length scale $u_0 = a_0 t_0^2 = a_0 / \omega_0^2$, Eqn.(4) can be simplified to:

$$\ddot{\psi}(\tau) + \frac{c_L}{m \omega_0} \dot{\psi}(\tau) + \frac{c_N}{m a_0^{1-\alpha} \omega_0^\alpha} \text{sgn}(\dot{\psi}(\tau)) |\dot{\psi}(\tau)|^\alpha + \psi(\tau) = -\lambda(\tau)\tag{5}$$

Eqn.(5) reveals that the non-dimensional displacement response of the system, $\psi(\tau)$, to the input $\lambda(\tau)$, is a function of only three non-dimensional parameters characteristic of the system:

$$\begin{aligned}\Pi_{c_L} &= \frac{c_L}{m \omega_0} \\ \Pi_{c_N} &= \frac{c_N}{m a_0^{1-\alpha} \omega_0^\alpha} \\ \Pi_\alpha &= \alpha\end{aligned}\tag{6a,b,c}$$

Parameter $\Pi_{c_L} = 2\xi$ describes dissipation capacity of the linear system and it is related to the inherent damping ratio ξ [8], parameter Π_{c_N} describes the damper dissipation capacity, and parameter $\Pi_\alpha = \alpha$ describes the damper non linearity. It is noteworthy that the choice of the dimensionless parameters is not unique. In fact, Π_{c_L} can be interchanged with ξ and Π_{c_N} can be substituted by other parameters measuring the total amount of nonlinear dissipation as well. For example, in [8] the damper dissipative property is described by the supplemental damping ratio ξ_d . This parameter is proportional to the ratio between the energy dissipated by the damper in an ideal cycle with amplitude equal to the peak displacement response u_{max} and circular frequency ω_0 , and the maximum elastic energy stored in the spring during the same cycle ([4][36][37]), and it can be expressed as

$$\xi_d = \frac{\lambda_\alpha}{\pi} \frac{c_N}{2m \omega_0} \omega_0^{\alpha-1} u_{max}^{\alpha-1}\tag{7}$$

where $\lambda_\alpha = \frac{2^{2+\alpha} \Gamma^2(1+\alpha/2)}{\Gamma(2+\alpha)}$ and where $\Gamma(\cdot)$ denotes the gamma function. The parameter λ_α equals π for $\alpha=1$ and 4 for $\alpha=0$ [4]. As already observed in [11], the definition of the parameter ξ_d involves not only the system parameters, but also the problem solution. Thus, differently from Π_{c_N} , ξ_d cannot be considered as a system characteristic parameter, but it can be useful to estimate dissipation properties exhibited for a particular seismic response. It is noteworthy that for $\alpha=1$, $\xi_d = \frac{\lambda_\alpha}{2\pi} \Pi_{c_N} = \frac{\Pi_{c_N}}{2}$ is independent on the response. Due to its physical meaning, the non-dimensional parameter $\Pi_{c_N}^* = \frac{\lambda_\alpha}{2\pi} \Pi_{c_N}$ will be used instead of Π_{c_N} in the parametric study discussed in the next section. It is worth to notice that the definition of the above introduced parameter $\Pi_{c_N}^* = \frac{\lambda_\alpha}{2\pi} \Pi_{c_N}$ coincides with the definition of the damper index (ε) used in [11] when a_0 coincides with the record peak ground acceleration.

It is important to observe that the normalized response of the dynamic system undergoing free vibrations or subjected to an impulsive input depends only on Π_{c_L} , Π_{c_N} , and Π_α . Differently, the seismic response depends also on the function $\lambda(\tau)$. Having assumed $1/t_0 = \omega_0$ as time scale, it follows that the expression of $\lambda(\tau)$ corresponding to a seismic input $\ddot{u}_g(t)$ imposed to a system with circular frequency ω_0 changes with ω_0 itself. Thus, the same seismic input $\ddot{u}_g(t)$ yields different non-dimensional response histories $\psi(\tau)$ and solutions, for systems with different frequency ω_0 . This observation has the important effect that also the system frequency ω_0 (or period $T = 2\pi / \omega_0$) has to be considered and varied in the following parametric study. In order to clarify this aspect, Fig.1 reports the time-histories of the non-dimensional displacement response $\psi(\tau)$ obtained for a system vibration period $T=1$ s and $T=2$ s, for the same set of the characteristic parameters $\Pi_{c_L} = 0.1$, $\Pi_\alpha = 0.3$ and $\Pi_{c_N} = 0.1$, under a ground motion record (Coalinga-01) of the PEER database [38]. The plots of Fig.1 confirm that the normalized system response changes with the system vibration period, even though the parameters Π_{c_L} , Π_{c_N} , Π_α are the same.

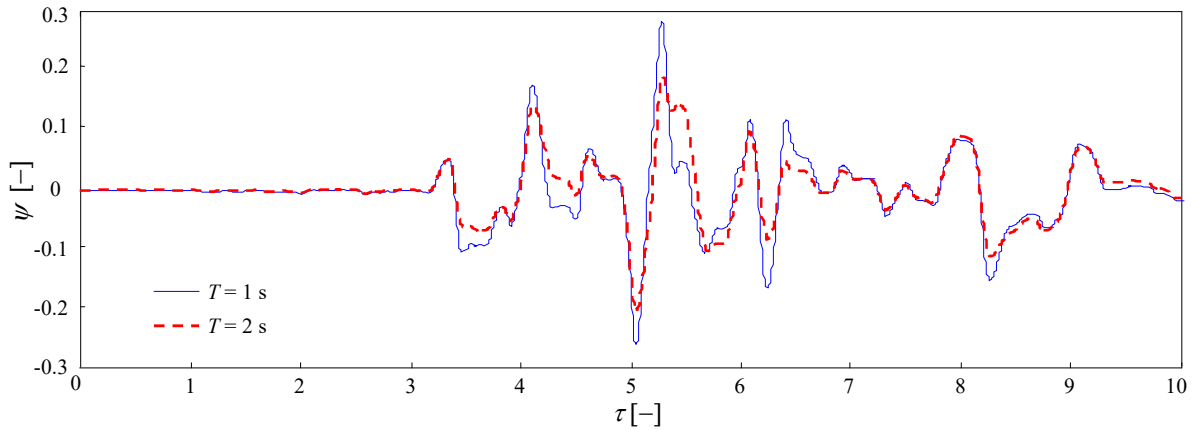


Fig. 1- Time-history of the dimensionless displacement response for a system natural period ($T=1$ s and $T=2$ s).

PARAMETRIC STUDY

Seismic response evaluation

In the seismic performance assessment of structural systems equipped with viscous dampers, two

important aspects need to be addressed. They concern the seismic input description and the choice of the parameters that have to be monitored to evaluate the system performance.

With reference to the first aspect, i.e. the seismic input description, in general an earthquake is characterized in terms of intensity, frequency content, and duration. These characteristics exhibit a significant degree of variability from record to record at a site, and need to be properly described and addressed. Coherently with the performance-based earthquake engineering (PBEE) approach [18]-[20], this study separates the uncertainties related to the seismic input intensity from those related to the characteristics of the record (record-to-record variability) by introducing a scale factor, a_0 , i.e. an intensity measure, through Eqn.(3). By this way, the randomness in the seismic intensity can be described by an hazard curve, whereas the ground motion randomness for a fixed intensity level can be described by selecting a set of ground motion realizations characterized by a different duration and frequency content, and by scaling these records to the common a_0 value.

In this study, the spectral pseudo-acceleration, $S_A(T, 5\%)$, at the fundamental period of the system, $T = 2\pi / \omega_0$, and for $\xi = 5\%$ (i.e., $\Pi_{c_L} = 10\%$), is assumed as intensity measure. The spectral pseudo-acceleration is related to the spectral displacement S_d by the relation $S_A(T, 5\%) = \omega_0^2 S_d(T, 5\%)$. It is worth to note that, in general, the intensity measure's choice should be driven by criteria of efficiency, sufficiency, and hazard computability [39]-[41]. At this regard, the assumed intensity measure is more efficient than the peak ground acceleration, thus it permits to reduce the response dispersion for the same number of ground motion considered and to obtain more confident response estimates for a given number of records employed [39]-[41]. Moreover, in this specific study, the choice of the assumed intensity measure is motivated by the fact that if all the records are normalized to $S_A(T, 5\%)$, then the displacement response of a SDOF system with period T , damping ratio $\xi = 5\%$, and without the supplemental damper becomes a constant, i.e., it is not affected by the record-to-record variability. Thus, the systems with no added damper can be assumed as reference cases for evaluating the influence of the added damper properties on the response dispersion.

With regard to the second topic, a set of response parameters relevant to the performance of the system components is considered in this study. This includes the peak relative displacement u_{\max} (related to internal forces in the structural frame, the stroke demand in the damper as well as to eventual displacement-sensitive non-structural components), the peak absolute acceleration a_{\max} (related to global forces on the system, i.e. the base shear, as well as to possible acceleration-sensitive non-structural components), and the peak internal force in the damper $f_{d,\max}$. These response parameters can be expressed in non-dimensional form as:

$$\begin{aligned}\eta_u &= \frac{u_{\max} \omega_0^2}{S_A(\omega_0, 5\%)} = \frac{u_{\max}}{S_d(\omega_0, 5\%)} \\ \eta_a &= \frac{a_{\max}}{S_A(\omega_0, 5\%)} \\ \eta_{f_d} &= \frac{f_{d,\max} / m}{S_A(\omega_0, 5\%)}\end{aligned}\tag{8a,b,c}$$

where the normalized displacement response η_u can be interpreted as the reduction factor of the 5% damped displacement response spectrum. It is noteworthy that based on η_u , the supplemental damping ratio, ξ_d , already defined via Eqn. (7), can also be expressed as:

$$\xi_d = \frac{\lambda_\alpha}{2\pi} \Pi_{c_N} \eta_u^{\alpha-1}\tag{9}$$

By repeatedly solving Eq.(5) for the set of ground motions records considered, a set of samples is obtained for each output variable that represents the response variability. In this paper, a probabilistic model based on a lognormal distribution, widely employed in PBEE ([18][19][40]), is used to describe the response. The assumption of lognormal distribution permits to estimate, even with a limited number of samples, the response at different percentile levels, which is very useful for the system reliability assessment. It also permits to obtain a closed-form analytical estimate of the risk [22]. A lognormal distribution can be fitted to the generic response parameter D (i.e., the extreme values $\eta_u, \eta_a, \eta_{fd}$ of Eq.(8)) by estimating the sample geometric mean, $GM(D)$, and the sample lognormal standard deviation $\sigma_{\ln}(D)$, or dispersion $\beta(D)$, defined as follows [18]:

$$GM(D) = \sqrt[N]{d_1 \cdot \dots \cdot d_N} \quad (10)$$

$$\beta(D) = \sigma_{\ln}(D) = \sqrt{\frac{(\ln d_1 - \ln[GM(D)])^2 + \dots + (\ln d_N - \ln[GM(D)])^2}{N-1}} \quad (11)$$

where d_i denotes the i -th sample value of D , N is the total number of samples. The sample geometric mean provides an estimate of the median of the response and its logarithm coincides with the lognormal sample mean $\mu_{\ln}(D)$. For small values, e.g., below 0.3, the dispersion $\beta(D)$ is approximately equal to the coefficient of variation of the distribution [22].

Parametric study results

This section shows the results of an extensive parametric study carried out to evaluate the relation between the damper properties and the system performance. In the study, the system period T is varied in the range between 0s and 4s, the parameter Π_α in the range between 0.15 and 1, whereas a constant value of 10% is assumed for Π_{c_L} (i.e., $\xi = 5\%$). The parameter Π_{c_N} is varied in order to

obtain values of $\Pi_{c_N}^* = \frac{\lambda_\alpha}{\pi} \Pi_{c_N}$ in the range between 0 and 0.30. It is recalled that $\Pi_{c_N}^*$ coincides with the supplemental damping ratio ξ_d for $\alpha=1$.

A set of 28 ground motions is considered in the parametric study to describe the record-to-record variability. The ground motions, reported in Table 1, have been selected from the PEER strong motion database [38] on the basis of three fundamental parameters: site class, source distance, and magnitude. Ground motions associated with site class B, as defined in Eurocode 8 [14], a source-to-site distance, R , greater than 10 km, and a moment magnitude, M_w , in the range between 6.0 and 7.5 are considered. The record number is deemed sufficient to obtain accurate response estimates, given the high efficiency of the intensity measure employed [39]-[41].

For each value of the parameters varied in the parametric study, the differential equation of motion, Eqn.(5), has been repeatedly solved for the different ground motion considered scaled to the common value of $S_A(\omega, 5\%)$. In particular, the Runge-Kutta-Fehlberg integration algorithm available in Matlab [45] has been employed for its ability of automatically adjusting the time-integration step size, thus improving the solution accuracy. The probabilistic properties of the response parameters have been evaluated by estimating the geometric mean, GM , and the dispersion, β , through Eqns. (10) and (11).

Fig. 2 shows the values of GM and β of the response parameters of interest, obtained for the different values of $\Pi_{c_N}^*$ and of T , and for $\Pi_\alpha=1$ (linear case). The results, already discussed in other studies (e.g., in [42][43]), are shown here because they provide a reference for comparing the results related to other values of Π_α and also because existing studies have not focused on the probabilistic aspects of the response.

Table 1. Selected ground motions for time history analysis (taken from [44]).

#	Earthquake	Station	Comp.	M _w	R (km)	Vs30(m/s)	PGA(m/s ²)
1	Coalinga-01	Parkfield - Gold Hill 4W	FN	6.36	41.1	438.3	0.119
2	Coalinga-01	Parkfield - Gold Hill 4W	FP	6.36	41.1	438.3	0.146
3	Coalinga-01	Parkfield - Vineyard Cany 6W	FN	6.36	40.9	438.3	0.106
4	Coalinga-01	Parkfield - Vineyard Cany 6W	FP	6.36	40.9	438.3	0.113
5	Morgan Hill	San Justo Dam (R Abut)	FN	6.19	31.9	622.9	0.135
6	Morgan Hill	San Justo Dam (R Abut)	FP	6.19	31.9	622.9	0.103
7	Loma Prieta	Fremont - Mission San Jose	FN	6.93	39.5	367.6	0.163
8	Loma Prieta	Fremont - Mission San Jose	FP	6.93	39.5	367.6	0.153
9	Loma Prieta	Palo Alto - SLAC Lab	FN	6.93	30.9	425.3	0.134
10	Loma Prieta	Palo Alto - SLAC Lab	FP	6.93	30.9	425.3	0.079
11	Big Bear-01	Joshua Tree	FN	6.46	41.9	379.3	0.093
12	Big Bear-01	Joshua Tree	FP	6.46	41.9	379.3	0.167
13	Northridge-01	Alhambra - Fremont School	FN	6.69	36.8	550	0.137
14	Northridge-01	Alhambra - Fremont School	FP	6.69	36.8	550	0.110
15	Northridge-01	Castaic - Old Ridge Route	FN	6.69	20.7	450.3	0.132
16	Northridge-01	Castaic - Old Ridge Route	FP	6.69	20.7	450.3	0.144
17	Northridge-01	LA - Brentwood VA Hospital	FN	6.69	22.5	416.6	0.130
18	Northridge-01	LA - Brentwood VA Hospital	FP	6.69	22.5	416.6	0.130
19	Northridge-01	LA - W 15th St	FN	6.69	29.7	405.2	0.154
20	Northridge-01	LA - W 15th St	FP	6.69	29.7	405.2	0.103
21	Chi-Chi Taiwan-06	CHY028	FN	6.3	33.6	542.6	0.123
22	Chi-Chi Taiwan-06	CHY029	FP	6.3	33.6	542.6	0.108
23	Chi-Chi Taiwan-04	CHY046	FN	6.2	38.1	442.1	0.140
24	Chi-Chi Taiwan-04	CHY047	FP	6.2	38.1	442.1	0.122
25	Chi-Chi Taiwan-06	TCU109	FN	6.3	37.9	424.2	0.131
26	Chi-Chi Taiwan-06	TCU110	FP	6.3	37.9	424.2	0.112
27	Chi-Chi Taiwan-06	TCU120	FN	6.3	32.5	459.3	0.126
28	Chi-Chi Taiwan-06	TCU121	FP	6.3	32.5	459.3	0.114

With reference to the geometric mean (Fig. 2a), it can be observed in general that for increasing damping the normalized displacements reduce, whereas the normalized damper forces increase. Also the absolute accelerations reduce for not too high vibration periods, but the reduction decreases for increasing damping values, whereas they increase for high damping values and high vibration periods. Moreover, for each value of $\Pi_{c_N}^*$, the normalized displacements reduce significantly for increasing T in the range 0s-0.3s, and they remain practically constant for increasing T in the range 0.3s-4s. The normalized damper forces always increase for increasing T , whereas the accelerations reduce for increasing T in the range between 0s and 1s, and slightly increase for increasing T in the range between 1s and 4s.

With reference to the response dispersion (Fig. 2b), it is worth to observe that for $\Pi_{c_N}^*=0$, the dispersion of the normalized displacements is null for all the vibration periods, in consequence of the intensity measure employed in this study. Obviously, also the dispersion of the damper forces is zero for $\Pi_{c_N}^*=0$, because the damper forces are identically null. The dispersion of the accelerations is close to zero, because the accelerations and pseudo-accelerations are very similar for low damping. As expected, the dispersion of all the response parameters increases by increasing $\Pi_{c_N}^*$, although for the linear case it remains quite low (below 0.3) and, as expected, it is practically insensitive to T . This is because the intensity measure employed accounts for the system period variation through the record scaling. Figs. 3-5 report the results for the nonlinear cases corresponding to $\Pi_{\alpha}=0.6, 0.3$ and 0.15 .

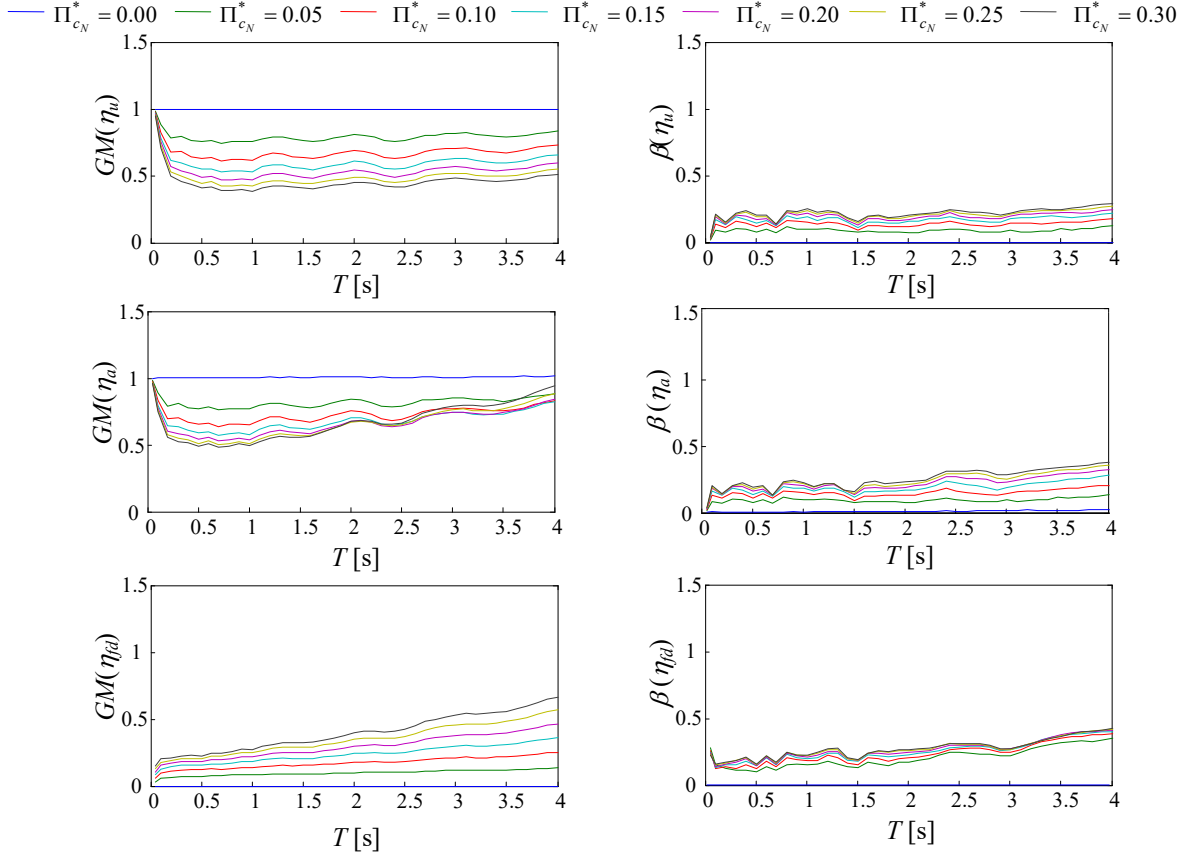


Fig. 2 - Sample geometric mean (a) and lognormal standard deviation (b) for $\Pi_\alpha = 1$.

For what concerns the geometric mean, similarly to the linear case, the highest reduction of displacements is attained for T close to 0.5s, for all the $\Pi_{c_N}^*$ and Π_α values. For a given $\Pi_{c_N}^*$ value, higher displacement response reductions are achieved by increasing the damper nonlinearity, i.e., for decreasing Π_α . Differently, the normalized damper forces exhibit different trends of variation with Π_α . In fact, for moderate periods they increase by increasing damper nonlinearity, whereas for large periods they decrease. For low Π_α values, the geometric mean of the damper forces is practically insensitive to the period. Finally, it can be noted that the normalized accelerations are not significantly influenced by variations of Π_α . This can be justified by the fact that the absolute accelerations are proportional to the sum of the forces in the damper and in the structure (proportional to η_u), which follow opposite trends for decreasing Π_α .

With reference to the response dispersion, it is worth to observe that $\beta(\eta_u)$ increases by increasing $\Pi_{c_N}^*$, similarly to the linear case, and it significantly increases for decreasing Π_α . Differently, the dispersion of the normalized forces, $\beta(\eta_{fd})$, follows an opposite trend, since it significantly decreases for decreasing Π_α . For $\Pi_\alpha = 0.15$, $\beta(\eta_{fd})$ is very low for all the values of $\Pi_{c_N}^*$ and this is coherent with the fact that for $\Pi_\alpha = 0$ the normalized damper forces would become deterministic. Finally, it is observed that the dispersion of the absolute accelerations, $\beta(\eta_a)$, similarly to the geometric mean, does not vary significantly by varying Π_α . This is again the effect of the opposite trends followed by the dispersion of the forces in the damper and in the structural system.

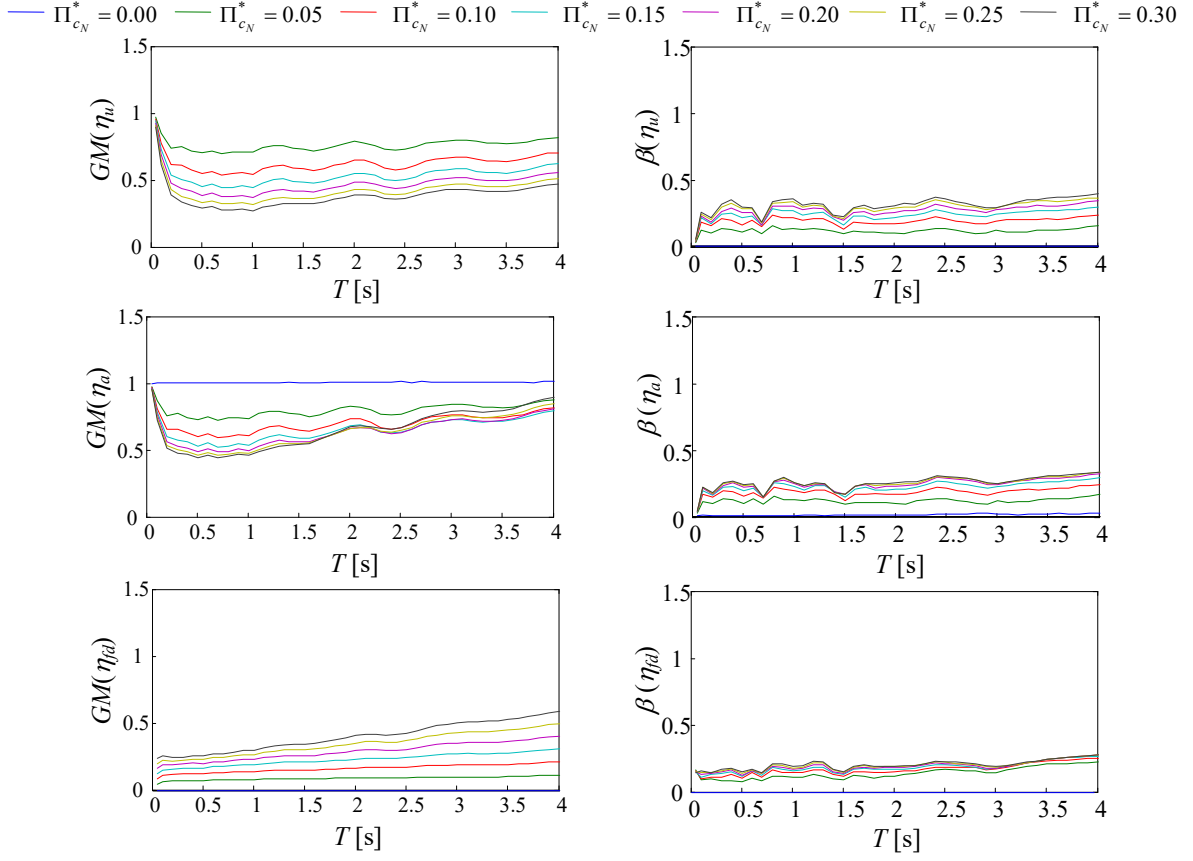


Fig. 3 - Sample geometric mean (a) and lognormal standard deviation (b) for $\Pi_\alpha = 0.6$.

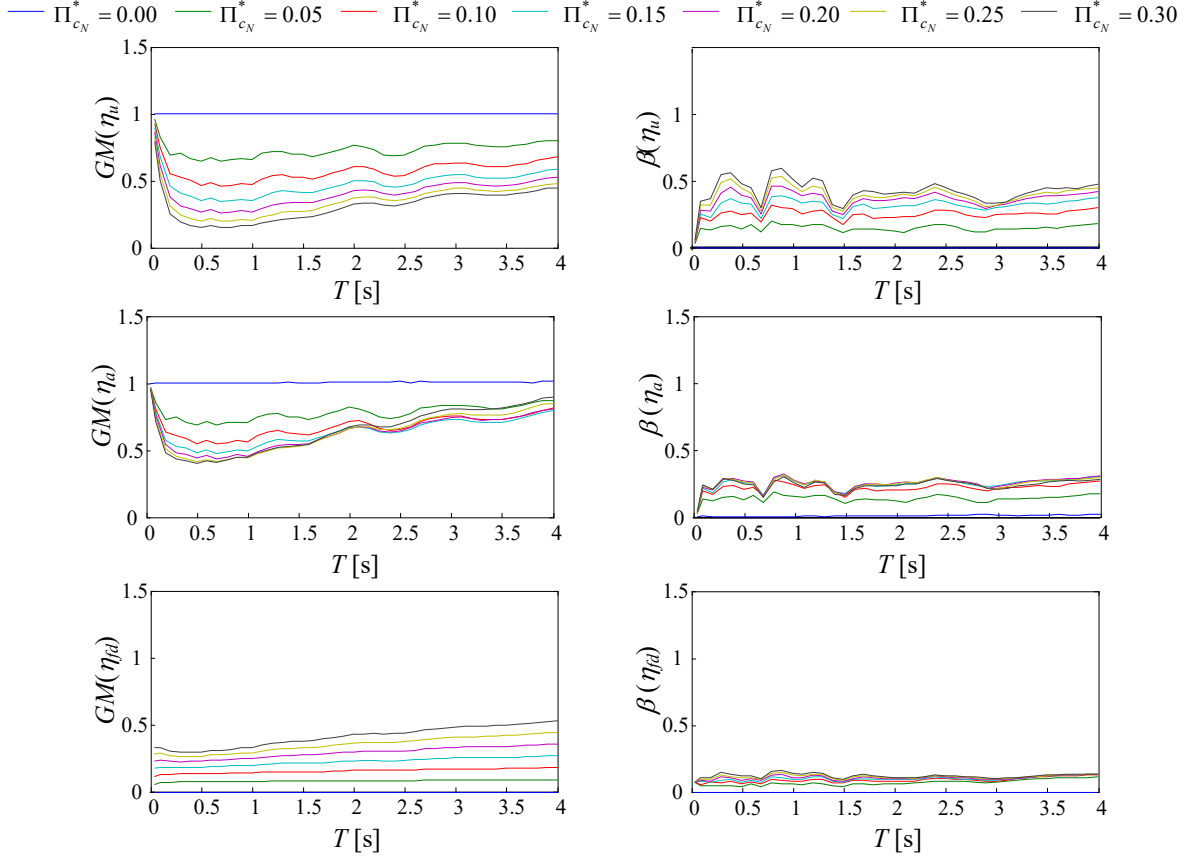


Fig. 4 - Sample geometric mean (a) and lognormal standard deviation (b) for $\Pi_\alpha = 0.3$.

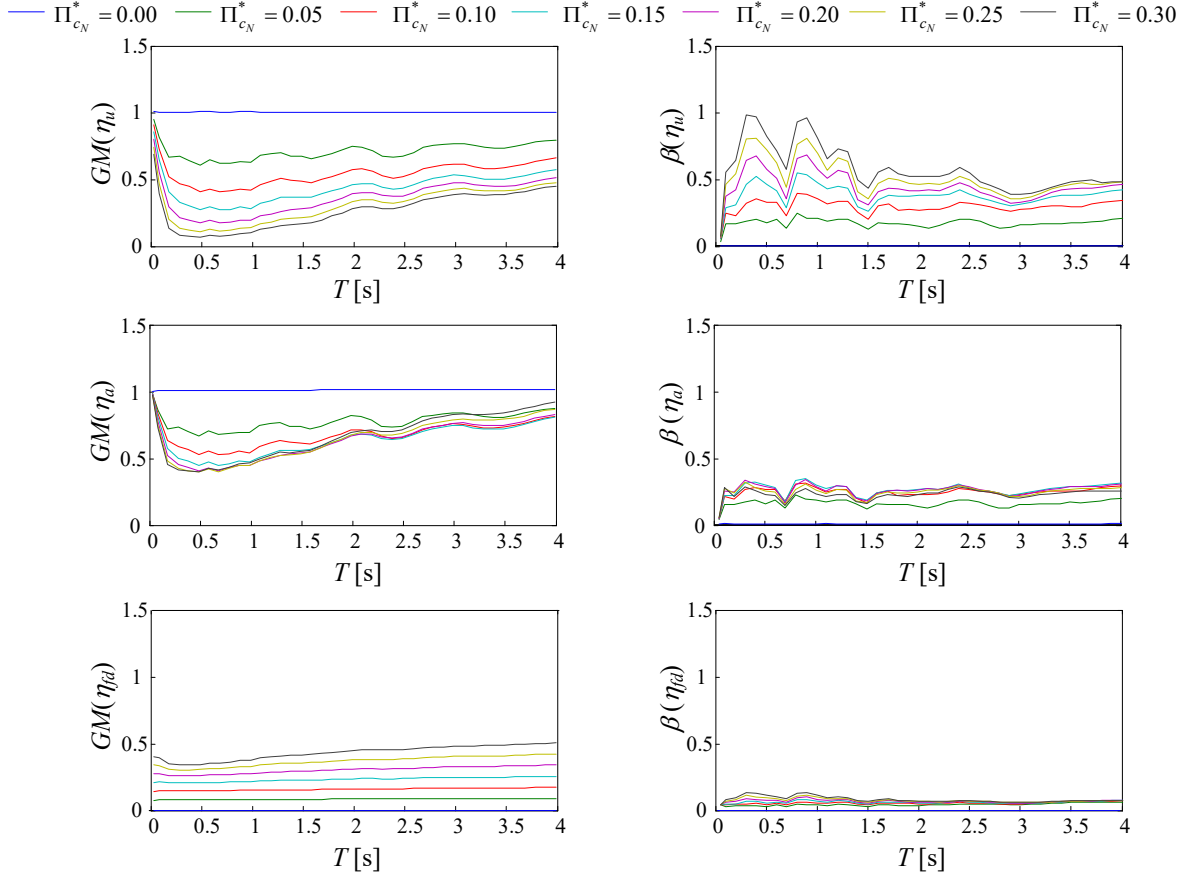


Fig. 5 - Sample geometric mean (a) and lognormal standard deviation (b) for $\Pi_\alpha = 0.15$.

In order to provide information regarding the dissipation capacity of the systems analyzed in the parametric study, the supplemental damping ratio ξ_d is plotted in Fig. 6, for each value of Π_α and of $\Pi_{c_d}^*$, as a function of the system period.

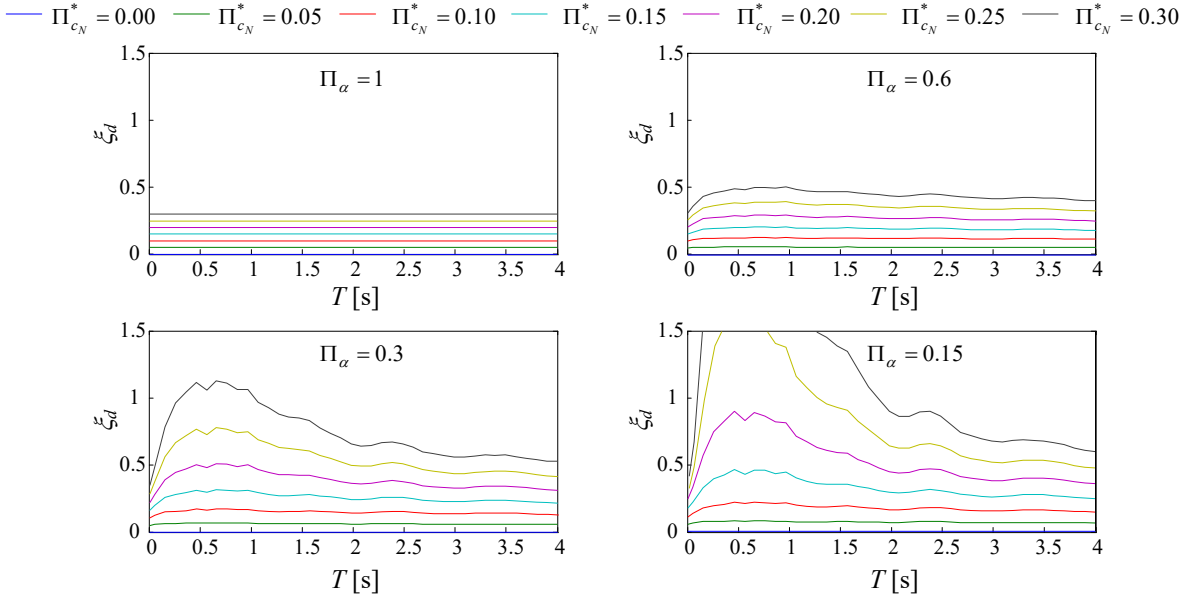


Fig. 6-Equivalent damping factors.

Of course, in the linear case, ξ_d coincides with $\Pi_{c_d}^*$ and does not vary with T . In the nonlinear case, ξ_d increases for increasing $\Pi_{c_d}^*$ and for decreasing Π_α . Thus, the dissipation capacity of a

damper characterized by a given value of $\Pi_{c_d}^*$ increases for increasing nonlinearity. Moreover, in the non linear cases, for a given value of $\Pi_{c_d}^*$, ξ_d increases for increasing T in the range between 0s and 0.5s, whereas it decreases for increasing T in the range between 0.5s and 4s. Finally, it is observed that for $\Pi_\alpha=0.15$, high values of $\Pi_{c_d}^*$ yield vary large values of ξ_d (even larger than 1), which are out of the range of design interest.

Since the lognormal distribution is employed in this study to describe the statistic of the various response parameters, an investigation has been carried out to evaluate whether it can provide a good fitting to the response samples. Some results of this investigation are reported hereinafter.

Fig. 7 reports and compares the empirical and fitted cumulative distributions of the samples of the response parameters obtained for a system with vibration period $T = 1$ s. Two cases are considered: one corresponds to $\Pi_{c_N}^* = 0.2$ and $\Pi_\alpha = 1$, involving a linear system behaviour, the other to $\Pi_{c_N}^* = 0.1$ and $\Pi_\alpha = 0.15$, involving a highly nonlinear behaviour. Both the cases correspond to a supplemental damping ratio of 20%. It can be seen that the fitted distribution is close to the empirical distribution in both the cases analyzed.

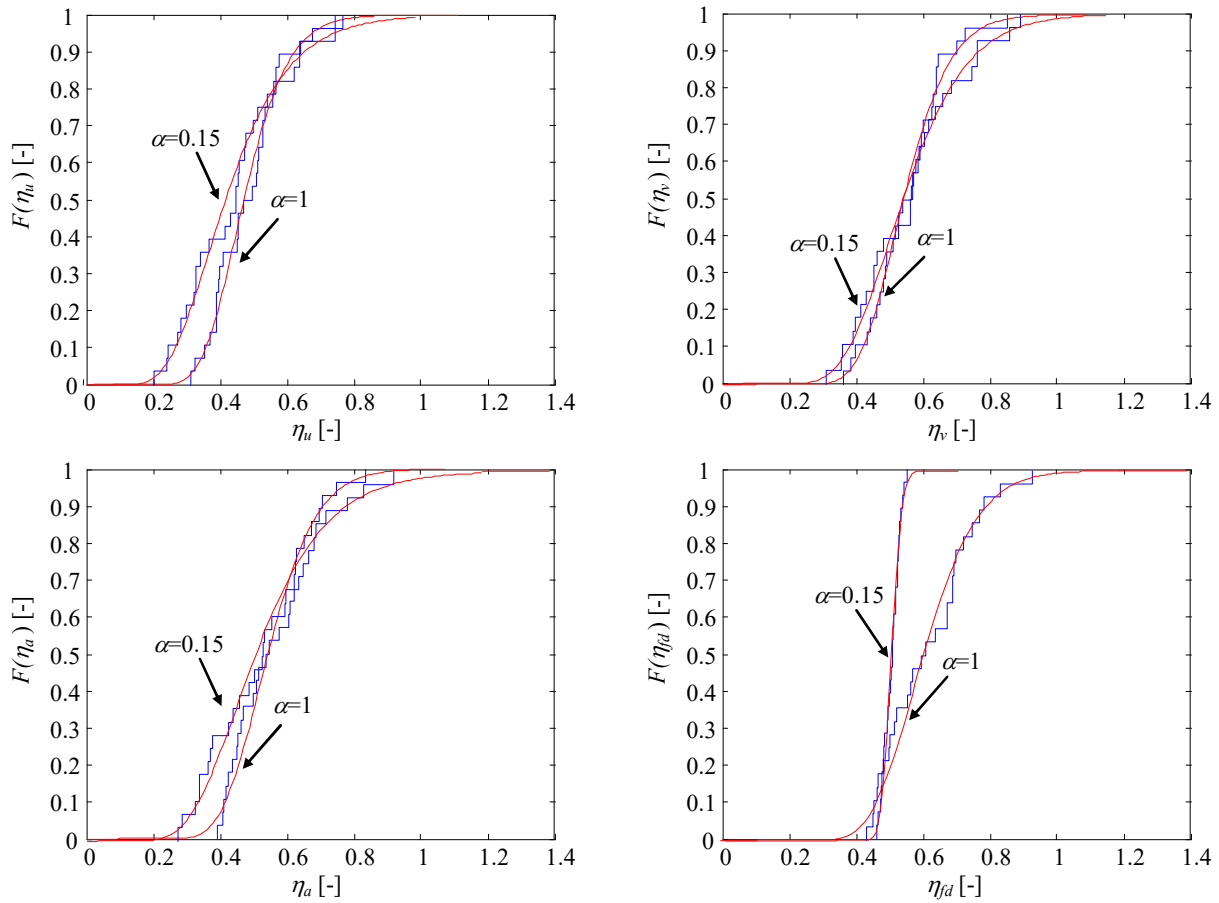


Fig. 7- Sample and fitted lognormal distribution of the response parameters of interest for $\alpha=1$ e $\alpha=0.15$.

In order to evaluate the suitability of the lognormal distribution, the Shapiro-Wilk parametric hypothesis test of normality has been carried out on the response samples of the various parameters analyzed [46]. This test, usually preferred to the Kolmogorov-Smirnov test in the case of small sample size (number of samples inferior than 50), returns a p-value, denoting the probability of rejecting the null hypothesis that the data come from a normal distribution when this hypothesis is true. A threshold equal to 0.05 is assumed for the p-values. This implies that for p-values inferior than 0.05, the lognormality assumption must be rejected. Table 2 reports the p-values obtained for

the various response parameters in the case corresponding to $T = 1$ s and for all the values of $\Pi_{c_N}^*$ and Π_α considered in the parametric analysis. In general, the lognormal distribution can be assumed to hold for all the response parameters of interest, even for a highly nonlinear and dissipative behaviour of the system (i.e., for low Π_α values and high $\Pi_{c_N}^*$ values). Similar results, not shown here due to space constraints, are observed for other system vibration periods.

Table 2 - p-values obtained for the various response parameters for different $\Pi_{c_N}^*$ and Π_α values and for $T = 1$ s

$\Pi_\alpha = 1$					$\Pi_\alpha = 0.6$				
$\Pi_{c_N}^*$	η_u	η_a	η_v	η_{f_d}	$\Pi_{c_N}^*$	η_u	η_a	η_v	η_{f_d}
0.05	0.3923	0.5177	0.8420	0.8420	0.05	0.5201	0.5089	0.7861	0.7861
0.1	0.8545	0.9690	0.4790	0.4790	0.1	0.7253	0.8300	0.2450	0.2450
0.15	0.8816	0.8669	0.2041	0.2041	0.15	0.8753	0.9580	0.5851	0.5851
0.2	0.8551	0.9820	0.3366	0.3366	0.2	0.8093	0.9668	0.7977	0.7977
0.3	0.	0.9708	0.4647	0.4647	0.3	0.4851	0.7467	0.5929	0.5929

$\Pi_\alpha = 0.30$					$\Pi_\alpha = 0.15$				
$\Pi_{c_N}^*$	η_u	η_a	η_v	η_{f_d}	$\Pi_{c_N}^*$	η_u	η_a	η_v	η_{f_d}
0.05	0.5713	0.6685	0.6379	0.6379	0.05	0.6420	0.7212	0.6348	0.6348
0.1	0.9514	0.9690	0.3665	0.3665	0.1	0.7539	0.8480	0.6833	0.6833
0.15	0.4758	0.7783	0.9196	0.9196	0.15	0.5181	0.6897	0.6961	0.6961
0.2	0.4846	0.7259	0.8117	0.8117	0.2	0.5844	0.6407	0.4115	0.4115
0.3	0.4355	0.5447	0.1991	0.1991	0.3	0.2796	0.7018	0.1519	0.1519

By assuming that the response parameters follow a lognormal distribution, the knowledge of the geometric mean and of the lognormal standard deviation, estimated from a limited number of the response samples through Eqns.(10) and (11), could be used to fully characterize their probability distribution function (PDF). In a lognormal distribution, the relation between the mean (μ_D) and the k -th percentile (d_k) of the generic demand D , can be expressed as:

$$d_k = \mu_D \exp \left[f(k) \beta(D) - \beta(D)^2 / 2 \right] \quad (12)$$

where $f(k)$ is a function assuming the values $f(50)=0$, $f(84)=1$ and $f(16)=-1$ [47]. However, it should be observed that p-values higher than 0.05 do not rigorously demonstrate that the response parameters are log-normally distributed, but only show that the available samples are consistent with the lognormality assumption. A more accurate description and fitting of the response in terms of PDF could be obtained only by using a very high number of records or different approaches (e.g., [31]-[33])

RELIABILITY OF SYSTEMS EQUIPPED WITH NONLINEAR VISCOUS DAMPERS

Previous section gives a general overview of the influence of the system and damper properties on the probabilistic seismic response, for values of the characteristic parameters in the range of interest for the design. In this section, the parametric study results are employed to evaluate and compare the reliabilities of a family of case studies involving viscous dampers with different nonlinear behavior designed to achieve the same performance target coherently with the approach of current seismic codes [14]-[17]. According to this approach, the design earthquake action is usually characterized by an intensity which corresponds to a pre-fixed exceedance probability or return

period (e.g. uniform hazard acceleration spectrum) [48]. The uncertainty in the seismic input at a given intensity level is accounted for by considering a set of records reflecting the record-to-record variability, and a “deterministic” measure of the performance is employed which usually coincides with the arithmetic mean of the response parameter samples obtained for the various records [18]. As it can be inferred from the results shown in the previous section, different couples of c_d and α can ensure the same deterministic performance objective. However, the probabilistic response properties may differ significantly from couple to couple.

Case study and seismic input description

The case studies considered in this section consist in a SDOF elastic system with natural vibration period $T = 1$ s and damping ratio $\xi = 5\%$, equipped with linear or nonlinear viscous dampers. The design earthquake action is characterized by an intensity which corresponds to a pre-fixed exceedance probability or return period (uniform hazard acceleration spectrum) [48]. A simplified hazard curve is assumed for the seismic input, as described by the following expression:

$$\nu(a_0) = 0.1046 \cdot a_0^{-2.8571} \quad (13)$$

where $\nu(a_0)$ denotes the mean annual frequency of exceeding the seismic intensity value a_0 . The hazard curve described by Eqn.(13) has been derived by following the procedure reported in [49], and is such that the value of the ultimate limit state (ULS) seismic intensity (with a probability of exceedance of 10% in 50 years) is $a_{0,ULS} = 0.4g$, whereas the value of the damage limitation state (DLS) seismic intensity (with a probability of exceedance of 10% in 10 years), is $a_{0,DLS} = 0.23g$. The definition of these two limit states is in accord with EC8 [14].

The viscous dampers are designed so that the mean peak displacement corresponding to the records of previous section scaled to the ULS intensity does not exceed the limit value of 0.04m. Since in the case of no added damper the mean peak displacement demand at the intensity $a_{0,ULS}$ is equal to 0.1m, the design objective corresponds to a target mean value of the displacement reduction factor η_u equal to 0.4. This design objective is achieved by considering different values of the damper velocity exponent α in the range 0.15-1.

Fig. 8a shows the design values of the damper size as measured by $\Pi_{c_N}^*$ that correspond to the target mean displacement reduction for the different α values considered, as obtained through interpolation of the results provided by the previous parametric study and reported in Figs. 2-5.

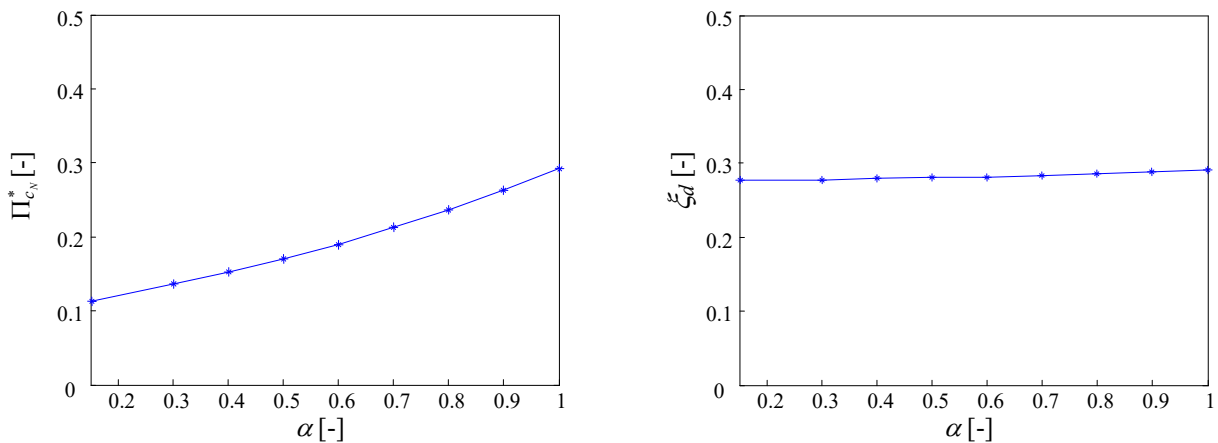


Fig. 8 – Values of the damper parameter ($\Pi_{c_N}^*$) and the supplemental damping ratio (ξ_d) for different values of α .

As expected, $\Pi_{c_N}^*$ decreases for decreasing α because the damper dissipation capacity for a given value of $\Pi_{c_N}^*$ increases by decreasing α (see Fig. 6). The values of $\Pi_{c_N}^*$ that ensure the design

objective for $\alpha=1$ and $\alpha=0.15$ are respectively 0.292 and 0.113, corresponding to values of the normalized damper constant respectively equal to $c_N/m = 3.669$ and $c_N/m = 0.785$. In Fig.8b, it is shown that the displacement reduction is mainly controlled by the supplemental damping ratio. In fact, very similar values of ξ_d are obtained (Eqn.(9)) for the different values of α considered.

Influence of damper non linearity on the probabilistic seismic response

In Fig. 9, the response properties obtained for the different damper nonlinearity levels are compared by plotting, vs. α , the sample mean, median, and the 84th and 16th percentiles of the normalized response parameters of interest at the design condition, as obtained via Eqn.(12). For what regards the "deterministic" performance, described by the mean response values, it can be observed that the normalized mean displacement is equal to 0.4 for all the α values considered. The mean normalized accelerations assume values of about 0.5 almost constant with α (the ratio between the absolute accelerations for $\alpha = 0.15$ and $\alpha=1$ is 1.06). Differently, the mean normalized force decreases significantly by reducing α . The ratio between the mean damper forces for $\alpha = 0.15$ and $\alpha=1$ is about 0.60. These "deterministic" results, also observed in other studies ([8][10]), confirm that the nonlinear viscous dampers permit to obtain on average displacement reductions similar to that achieved with a linear viscous damper while limiting significantly the damper force and without increasing significantly the absolute accelerations.

For what regards the probabilistic performance, synthetically described by the median and the 84th and 16th percentiles of the normalized response parameters of interest, it can be observed in Fig. 9 that in general the median response values are close to the corresponding mean values, with normalized differences below 15%. This is expected, given the reduced response dispersion. Differently, the 16th and 84th percentiles are significantly different from the corresponding median values, and the difference varies with α and with the response parameter considered.

In particular, the difference between the 16th and 84th percentile of the displacement response and the median value increases by increasing α , in consequence of the increased dispersion, as measured by β_u . A similar trend is observed for the absolute accelerations percentiles, whereas an opposite trend is observed for the 16th and 84th percentiles of the damper force. In fact, the force percentiles tend to the median value when α decreases in consequence of the decreasing dispersion β_{f_d} . This result may impact the damper sizing, which is usually governed by the stroke (proportional to u) and the force that have to be withstood. For example, for $\alpha = 1$, the 84th percentile of the normalized displacement is $\eta_{u,84} = 0.498$ (i.e., 1.25 times the corresponding mean value), whereas the 84th percentile of the normalized damper force is $\eta_{f_d,84} = 0.336$ (i.e., 1.22 times the corresponding mean value). For $\alpha = 0.15$, $\eta_{u,84} = 0.549$ (i.e., 1.37 times the corresponding mean value) and $\eta_{f_d,84} = 0.175$ (i.e., 1.05 times the corresponding mean value). Given their importance in ensuring the safety and reliability of the whole system, it is fundamental to design the dampers (both the damper components and the connections to the structure) with a know level of reliability, which could be even higher than the reliability level of the structure to be protected. This goal may be achieved by proposing amplifying factors depending on the exponent α of the constitutive law, as also suggested in Annex E of EN15129 for the damper forces [50].

Although the viscous dampers are usually designed so that the protected structure satisfies a specific performance objective for a given seismic intensity, the response of the system at different (smaller and larger) seismic intensities needs to be evaluated. With reference to the case studies analyzed in this section, the response parameters of interest (mean, median and 84th and 16th percentiles values) are evaluated also for seismic intensities other than the ULS intensity $a_{0,ULS}$ considered for the damper design. As observed previously, this requires recalculating the values of the non-dimensional characteristic parameters reported in Eqn. 6 and exploiting the parametric study results reported in Figs. 2-5.

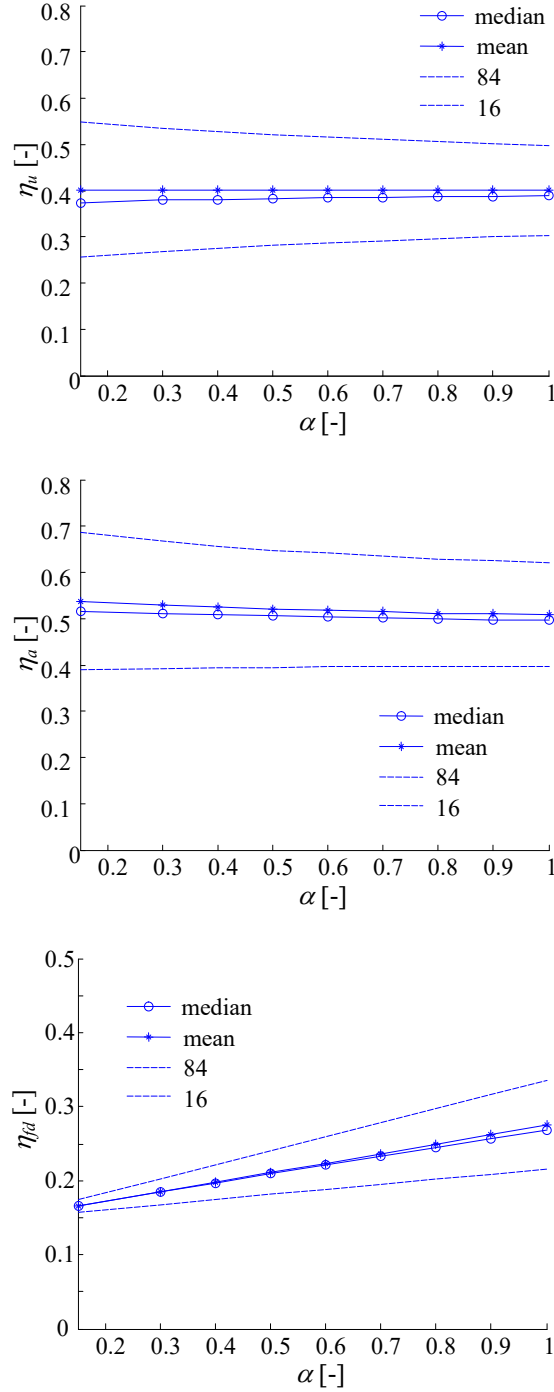


Fig. 9 – Normalized response parameters for different values of α .

Fig. 10 plots the variation with a_0 of the system displacement response and of the damper force corresponding to the damper exponents $\alpha = 0.15$ and $\alpha = 1$. The response parameters are here reported in dimensional form so that the plots of Fig. 10 may also be interpreted as summarized incremental dynamic analysis curves. Obviously, the mean displacement curves for $\alpha = 0.15$ and $\alpha = 1$ pass through the design displacement $u_d = 0.04\text{m}$ at the design intensity $a_{0,ULS} = 0.4\text{g}$, whereas the mean values of the damper force are significantly different and they are $f_d = 490.64\text{ kN}$ and $f_d = 295.16\text{ kN}$ in the linear and nonlinear case respectively.

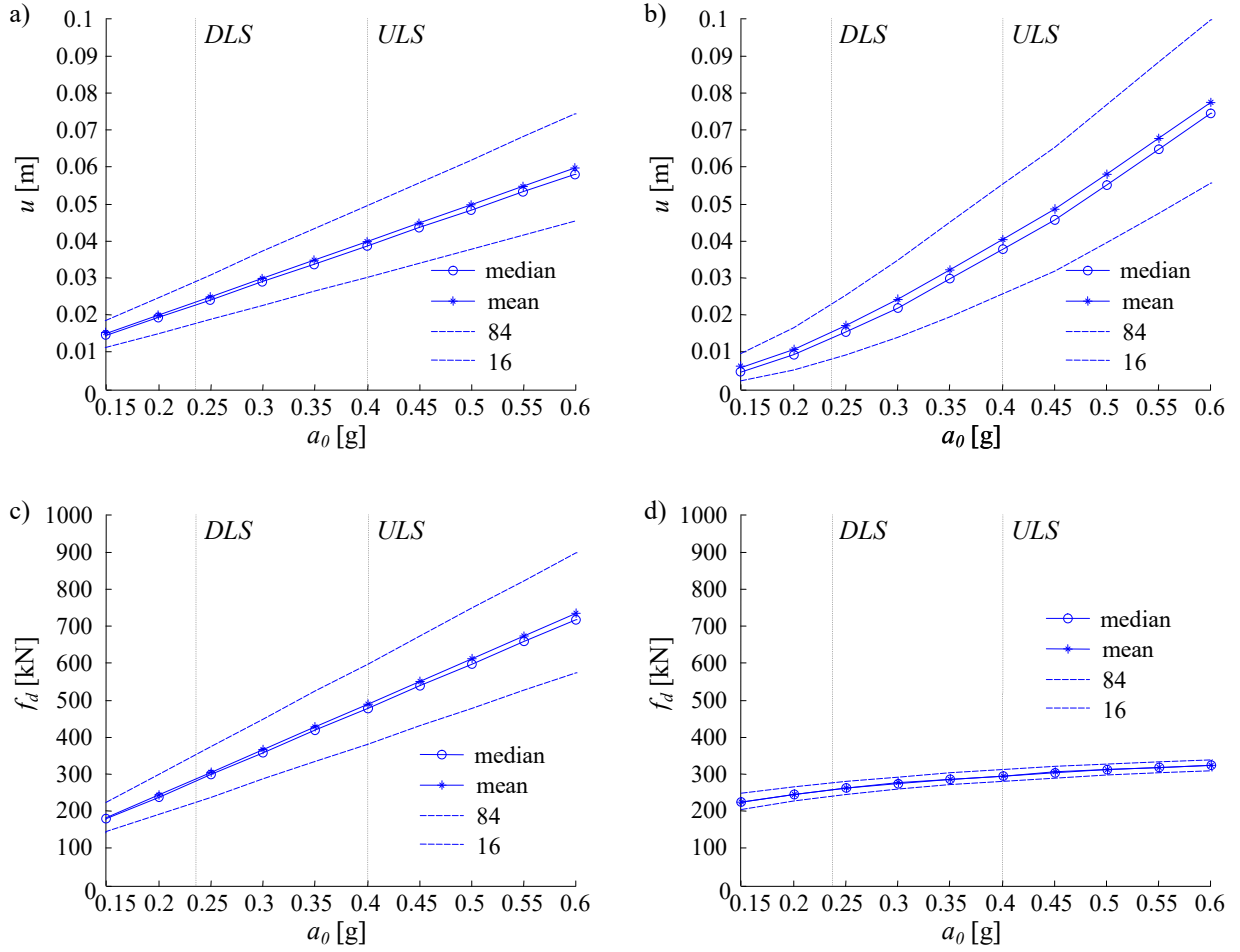


Fig. 10 – Variation with a_0 of the displacement demand for $\alpha = 1$ (a) and $\alpha = 0.15$ (b) and of the force demand for $\alpha = 1$ (c) and $\alpha = 0.15$ (d).

As expected, in the case corresponding to $\alpha = 1$ the response varies linearly with a_0 . Thus, the mean displacement and damper force demand reduce by a factor $0.23/0.4 = 0.575$ by passing from the ULS to the DLS intensity. On the other hand, in the nonlinear case corresponding to $\alpha = 0.15$, the mean displacement demand increases more than linearly with a_0 whereas the mean damper force demand increases less than linearly. This implies that for low seismic intensities, the displacement demand obtained with the nonlinear damper is smaller than that obtained with the linear damper, while the value of the damper force normalized with respect to the design ULS value is higher. In particular, at the DLS intensity level, $a_{0,DLS}$, the displacement for $\alpha = 1$ is about 0.023m, whereas for $\alpha = 0.15$ it is about 0.01 m. This can also be explained by noting that the supplemental damping ratio of the nonlinear viscous damper is significantly higher than that of the linear viscous damper for seismic intensities lower than $a_{0,ULS}$. On the other hand, the ratio between the mean damper force at the DLS and ULS intensity (0.575 in the linear case) is 0.88 in the nonlinear case. Opposite considerations hold for seismic intensities larger than the design ULS intensity (e.g., for the collapse limit state intensity): the displacement demand obtained with the nonlinear damper is larger than that obtained with the linear damper, while the value of the damper force normalized with respect to the design ULS value is significantly lower. The plots of the values of $\Pi_{c_N}^*$ and of the corresponding ξ_d for the different seismic intensity levels are reported in Fig.11.

With regard to the probabilistic response, while in the linear case the response dispersion is constant, in the nonlinear case it varies significantly with a_0 , as it can be better inferred from Fig. 12 where the variation with a_0 of the displacement and damper force dispersion is reported. In particular, the displacement response dispersion is very high for low a_0 values, and it decreases for increasing a_0 ,

whereas the dispersion of the damper forces is in general very low and it also decreases with a_0 . At the intensity level $a_{0,DLS}$, in the linear case the displacement and force dispersions are the same as those evaluated at $a_{0,ULS}$, whereas in the nonlinear case the displacement dispersion is significantly higher and the force dispersion is slightly lower than the corresponding dispersion at $a_{0,ULS}$.

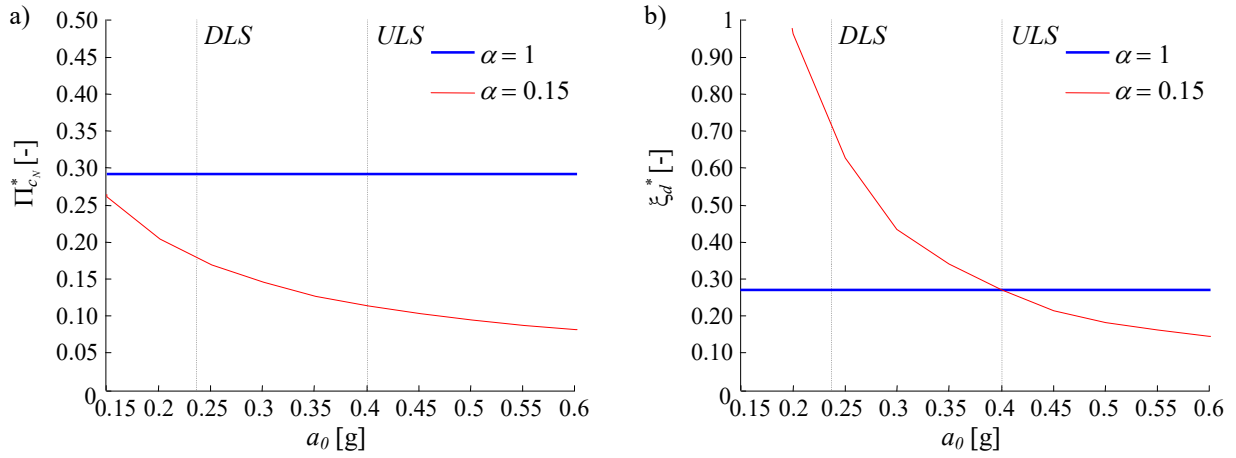


Fig. 11 – Variation with a_0 of the values of $\Pi_{c_N}^*$ (a) and of ξ_d^* (b) at the design condition.

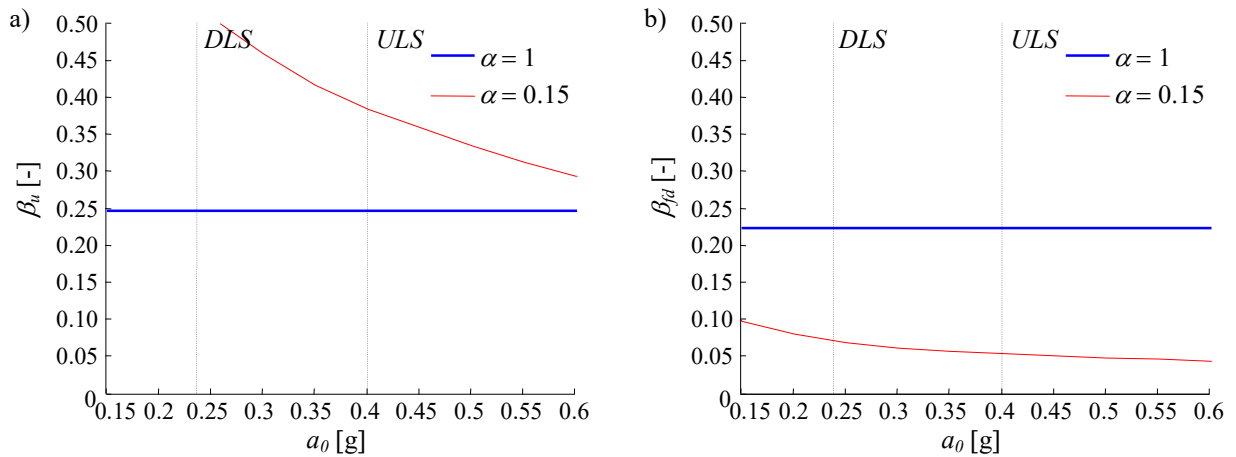


Fig. 12 – Variation with a_0 of the displacement and damper force dispersion.

Influence of damper non-linearity on the seismic risk

In order to shed light on the effects of the damper nonlinear behaviour and of the response dispersion on the seismic reliability of the system, the risk of exceeding reference values of the displacements and of the forces during a life-time of $T_L=50$ yrs is computed. In particular, in order to highlight possible limitation of current deterministic approaches, the mean values of the response parameter of interest are assumed as reference values and both the deterministic (mean) and the probabilistic response are considered as demand models. More specifically, the reference value of the displacement is assumed equal to the target displacement of 0.04m for both the cases of the linear and nonlinear damper. The reference value of the force is assumed equal to the mean value of the damper force obtained for the various records at the seismic intensity $a_{0,ULS}$, i.e., 490.64 kN for $\alpha = 1$, and 295.16 kN for $\alpha = 0.15$. The risk P_{D,T_L} that the uncertain demand D of displacement/force exceeds the corresponding reference value d^* during the time T_L is obtained by assuming a poissonian occurrence of the exceedance events as follows [49]:

$$P_{D,T_L} = P(D \geq d^*) = 1 - \exp[-v_D(D \geq d^*)T_L] \quad (14)$$

where $v_D(D \geq d^*)$ is the mean annual frequency of exceedance of the demand, expressed as:

$$v_D(D \geq d^*) = \int_0^\infty P_D(a_0) \cdot |dv(a_0)| \quad (15)$$

The expression of $v(a_0)$ is given by Eqn.(13), and $P_D(a_0) = P(D \geq d^* | a_0)$ denotes the probability of exceedance conditional on the seismic intensity level a_0 . The displacement and force exceedance probabilities conditional to a_0 are plotted as continuous lines in Fig.13 and they can be interpreted to as fragility or vulnerability curves. These curves are derived by comparing, for each value of a_0 , the lognormally distributed demand (Fig. 10) with the corresponding reference value. In Fig. 13, also the stepwise fragility curve corresponding to the deterministic demand model is reported for comparison. It is worth to observe that, since for a lognormally distributed variable the mean value is always larger than the median value (see Fig. 10), at the design seismic intensity $a_{0,ULS}$ the conditional probabilities of failure obtained by adopting a probabilistic demand model are lower than 0.5 (the scatter is controlled by the dispersion, according to Eqn.(12), and it tails off when the dispersion decreases). This implies a local difference at $a_{0,ULS}$ between the fragility curves of the linear and non linear case, as more evident in the case of damper forces (Fig. 13b). For what concerns the displacements, the difference between the fragility curves (Fig.13a) is notable only for $a_0 > 0.4g$ and this is mainly due to the displacement demand in the nonlinear case that increases more than linearly by increasing the seismic intensity (see Fig.10b).

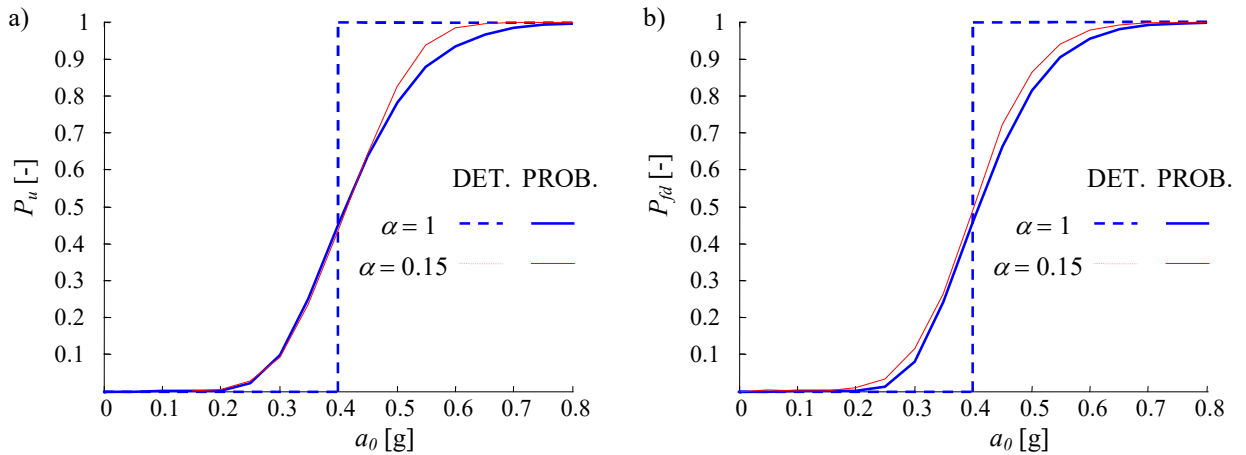


Fig. 13 – Variation with a_0 of the probability of exceeding the design value of the displacement (a) and of the damper force (b) according to the deterministic and the probabilistic approach.

Table 3 reports the probabilities of exceeding the reference values of the displacement and of the force during $T_L=50$ yrs according to the deterministic and the probabilistic demand model, for both the cases of the linear and nonlinear damper. It is noteworthy that according to the deterministic approach, the probability of exceeding the reference values of the demand is equal to the probability of exceeding the design intensity $a_{0,ULS}$.

The risk estimates obtained with the probabilistic approach are always higher than the corresponding estimates obtained with the deterministic demand model based on the mean response values. In particular, the risk increases up to 20% for the displacements and to 50% for the damper forces by passing from the deterministic to the probabilistic approach. This is mainly the effect of the response dispersion, which increases the exceedance probability at low seismic intensities characterized by a high probability of occurrence.

Also some differences can be observed between the risk estimates obtained for the case of the linear and nonlinear damper by employing the probabilistic approach. In particular, the risk of exceeding the displacement reference value is only slightly higher for the nonlinear damper. In fact, the fragility curve for $\alpha = 0.15$ assumes higher values compared to the fragility curve for $\alpha = 1$ only at high seismic intensities (Fig. 10), which have a low probability of occurrence and thus provide a negligible contribution to the risk. On the other hand, the risk of exceeding the damper force

reference value is significantly higher for the nonlinear case than for the linear case because of the higher vulnerability observed in Fig. 10 for all the α_0 values.

Table 3 - risk estimates according to the deterministic and probabilistic approach

Risk	Probabilistic approach		Deterministic approach	
	$\alpha = 1$	$\alpha = 0.15$	$\alpha = 1$	$\alpha = 0.15$
$P_{u,50}$ [-]	0.1138	0.1212	0.1000	0.1000
$P_{f_d,50}$ [-]	0.1112	0.1478	0.1000	0.1000

CONCLUSIONS

This paper analyzes the probabilistic characteristics of the seismic response of structural systems equipped with linear/nonlinear viscous dampers by considering a simple single-degree-of-freedom linear structural system.

Firstly, the characteristic parameters that control the system dynamic behaviour and seismic response are found by carrying out the non-dimensionalization of the equation of motion. These include the two non-dimensional parameters that describe the damper dissipative capacity and nonlinear behaviour. Then, an extensive parametric study is carried out to evaluate the influence of the damper properties on the probabilistic response (geometric mean and dispersion) under a set of natural ground motions describing the record-to-record variability, for a wide range of variation of the characteristic parameters.

The parametric study results are used to study the influence of the damper properties, in particular the velocity exponent controlling the non linear behavior, on the seismic reliability of systems equipped with nonlinear viscous dampers. To this purpose, the probabilistic responses of a family of case studies, involving dampers with different nonlinear behavior and designed according to the same deterministic performance target, are evaluated and compared. This performance target coincides with the mean displacement demand at the ultimate limit state (ULS) seismic intensity. Based on the results of this investigation, the following conclusions can be drawn. 1) At the ULS intensity, the family of case studies considered is characterized by a displacement dispersion higher in the nonlinear case than in the linear case, whereas the damper force dispersion is significantly lower in the nonlinear case than in the linear case. The dispersion of the normalized accelerations does not significantly depend on the damper nonlinearity level. 2) For increasing seismic intensities, in the case of nonlinear dampers the displacement demand increases more than linearly, whereas the damper forces increase less than linearly. Also the response dispersion varies significantly with the seismic intensity. In particular, the dispersion of the displacement response is very high for low seismic intensities, and it decreases for increasing intensities, whereas the dispersion of the damper forces is in general very low and it decreases for increasing intensities. 3) The nonlinear dampers provide higher reduction of the mean displacement response than the linear damper at the damage limit state seismic intensity. Also the response dispersion is higher for the nonlinear damper. 4) The deterministic code approach for the seismic assessment/design of structures yields risk estimates lower than the corresponding estimates obtained through a probabilistic approach. Furthermore, the safety levels observed in solutions obtained by a conventional deterministic design vary by varying the damper exponent and significant differences can be observed between displacements and forces.

REFERENCES

- [1] Soong TT, Dargush GF. *Passive Energy Dissipation Systems in Structural Engineering*. Wiley: New York, 1997.
- [2] Symans MD, Charney F, Whittaker A, Constantinou M, Kircher C, Johnson M, McNamara R. *Energy Dissipation Systems for Seismic Applications: Current Practice and Recent Developments*. *Journal of Structural Engineering* 2008; **134**(1): 3-21.
- [3] Christopoulos C, Filiatrault A. *Principles of Passive Supplemental Damping and Seismic*

Isolation. IUSS Press: Pavia, Italy, 2006.

- [4] Symans MD, Constantiou MC. Passive fluid viscous damping systems for seismic energy dissipation. *ISET Journal of Earthquake Technology* 1998; **35**(4):185-206.
- [5] Lee D, Taylor DP. Viscous damper development and future trends. *The Structural Design of Tall Buildings* 2001; **10**(5): 311-320.
- [6] Hwang J, Tsai C, Wang S, Huang Y. Experimental study of RC building structures with supplemental viscous dampers and lightly reinforced walls. *Engineering Structures* 2006; **28**(13): 1816-1824.
- [7] Peckan G, Mander JB, Chen SS. Fundamental Considerations for the design of non-linear viscous dampers. *Earthquake Engineering and Structural Dynamics* 1999; **28**(11): 1405-1425.
- [8] Lin WH, Chopra AK. Earthquake response of elastic SDF systems with non-linear fluid viscous dampers. *Earthquake Engineering and Structural Dynamics* 2002; **31**(9): 1623-1642.
- [9] Denoel V, Degee H. Analysis of linear structures with non linear dampers. *Proceedings of the 5th International conference on Structural dynamics EUROdyn 2002*, Munich, Germany, 2-5 September 2002.
- [10] Martinez-Rodrigo M, Romero ML. An optimum retrofit strategy for moment resisting frames with nonlinear viscous dampers for seismic applications. *Engineering Structures* 2003; **25**(7): 913–925.
- [11] Diotallevi PP, Landi L, Dellavalle A. A methodology for the direct assessment of the damping ratio of structures equipped with nonlinear viscous dampers. *Journal of Earthquake Engineering* 2012; **16**(3):350-373.
- [12] Zhang J, Xi W. Optimal Nonlinear Damping for Inelastic Structures Using Dimensional Analysis. *Proceedings of the 20th Analysis and Computation Specialty Conference*, Chicago, 2012.
- [13] Bahnasy A, Lavan O. Linear or Nonlinear Fluid Viscous Dampers? A Seismic Point of View. *Proceedings of the Structures Congress*, Pittsburgh, 2013.
- [14] European Committee for Standardization. Eurocode 8—Design of Structures for Earthquake Resistance. Part 1: General Rules, Seismic Actions and Rules for Buildings, Brussels, 2004.
- [15] FEMA-368. NEHRP recommended provisions for seismic regulations for new buildings and other structures, 2000 Edition, Part 1, Washington DC, 2000.
- [16] NZS 1170.5. Structural design actions, Part 5: Earthquake actions - New Zealand. Standards New Zealand, Wellington, NZ, 2004.
- [17] American Society of Civil Engineers (ASCE). *Minimum design loads for buildings and other structures*, Reston, VA, 2006.
- [18] Bradley BA. Design Seismic Demands from Seismic Response Analyses: A Probability-Based Approach. *Earthquake Spectra* 2011; **27**(1): 213-224.
- [19] Aslani H, Miranda E. Probability-based seismic response analysis. *Engineering Structures* 2005; **27**(8): 1151-1163.
- [20] Porter KA. An overview of PEER's performance-based earthquake engineering methodology. *Proceedings, Proceedings of the 9th International Conference on Application of Statistics and Probability in Civil Engineering (ICASP9)*, San Francisco, California, 2003; 973-980.
- [21] Zhang Y, Acero G, Conte J, Yang Z, Elgamal A. Seismic Reliability Assessment of a Bridge Ground System. *Proceedings of the 13th World Conference on Earthquake Engineering*, Vancouver, Canada, 2004.
- [22] Cornell C, Jalayer F, Hamburger R, Foutch D. Probabilistic Basis for 2000 SAC Federal Emergency Management Agency Steel Moment Frame Guidelines. *Journal of Structural*

Engineering 2002; **128**(4): 526-533.

- [23] Hamburger R. The ATC-58 Project: Development of Next-Generation Performance-Based Earthquake Engineering Design Criteria for Buildings. *Proceedings of the Structures Congress*, St. Louis, MO, 2006.
- [24] Marano GC, Trentadue F, Greco R. Stochastic optimum design criterion for linear damper devices for seismic protection of buildings. *Structural Multidisciplinary Optimization* 2007; **33**(6): 441-455.
- [25] Smyth A, Altay G, Deodatis G, Erdik M, Franco G, Gülkan P, Kunreuther H, Luş H, Mete E, Seeber L, Yüzügüllü O. Probabilistic Benefit-Cost Analysis for Earthquake Damage Mitigation: Evaluating Measures for Apartment Houses in Turkey. *Earthquake Spectra* 2004; **20**(1): 171-203.
- [26] Güneyisi EM, Altay G. Seismic fragility assessment of effectiveness of viscous dampers in R/C buildings under scenario earthquakes. *Structural Safety* 2008; **30**(5): 461-480.
- [27] Özel AE, Güneyisi EM. Effects of Eccentric Steel Bracing Systems on Seismic Fragility Curves of Mid-Rise Reinforced Concrete Buildings: A Case Study. *Structural Safety* 2011; **33**(1): 82-95.
- [28] Güneyisi EM. Seismic Reliability of Steel Moment Resisting Framed Buildings Retrofitted with Buckling Restrained Braces. *Earthquake Engineering and Structural Dynamics* 2012; **41**(5): 853-874.
- [29] Freddi F, Tubaldi E, Ragni L, Dall'Asta A. Probabilistic performance assessment of low-ductility reinforced concrete frames retrofitted with dissipative braces. *Earthquake Engineering and Structural Dynamics* 2013; **42**(7): 993-1011.
- [30] Lavan O, Avishur M. Seismic behavior of viscously damped yielding frames under structural and damping uncertainties. *Bulletin of Earthquake Engineering* 2013; **11**(6): 2309-2332.
- [31] Di Paola M, La Mendola L, Navarra G. Stochastic seismic analysis of structures with nonlinear viscous dampers. *Journal of Structural Engineering* 2007; **133**(10): 1475-1478.
- [32] Barone G, Navarra G, Pirrotta A. Probabilistic response of linear structures equipped with nonlinear dampers devices (PIS method). *Probabilistic engineering mechanics* 2008, **23**(2): 125-133.
- [33] Peng Y, Mei Z, Li J. Stochastic seismic response analysis and reliability assessment of passively damped structures. *Journal of Vibration and Control* 2013, early view.
- [34] Tubaldi E, Kougiumtzoglou IA. Nonstationary stochastic response of structural systems equipped with nonlinear viscous dampers under seismic excitation. *Earthquake Engineering and Structural Dynamics* 2013, under review.
- [35] Gockenbach MS. Partial Differential Equations, Analytical and Numerical Methods (2nd edn). Siam: Philadelphia, 2011.
- [36] Jacobsen LS. Steady forced vibrations as influenced by damping. *ASME Transactions* 1930; **52**(1): 169-181.
- [37] Chopra AK. Dynamics of Structures: Theory and Applications to Earthquake Engineering (2nd edn). Prentice-Hall: Upper Saddle River, NJ, 2001.
- [38] Pacific Earthquake Engineering Center (PEER). PEER strong motion database, 2006. (<http://peer.berkeley.edu/smcat>).
- [39] Pinto PE, Giannini R, Franchin P. Seismic Reliability Analysis of Structures, IUSS Press, Pavia, Italy, 2003.
- [40] Shome N, Cornell CA, Bazzurro P, Carballo JE. Earthquake, records, and nonlinear responses. *Earthquake Spectra* 1998; **14**(3): 469-500.
- [41] Luco N, Cornell CA. Structure-specific scalar intensity measures for near-source and ordinary

earthquake ground motions. *Earthquake Spectra* 2007; **23**(2): 357-92.

- [42] Sadek F, Mohraz B, Riley M. Linear procedures for structures with velocity-dependent dampers. *Journal of Structural Engineering* 2000; **126**(8): 887-895.
- [43] Lin Y, Chang K. Effects of site classes on damping reduction factors. *Journal of Structural Engineering* 2004; **130**(11): 1667-1675.
- [44] Zona A, Ragni L, Dall'Asta A. Sensitivity-based study of the influence of brace over-strength distributions on the seismic response of steel frames with BRBs. *Engineering Structures* 2012; **37**(1): 179-192.
- [45] Math Works Inc. MATLAB-High Performance Numeric Computation and Visualization Software. User's Guide. Natick: MA, USA, 1997.
- [46] Shapiro SS, Wilk MB. An analysis of variance test for normality (complete samples). *Biometrika* 1965; **52**(3-4): 591-611.
- [47] Ang AHS, Tang WH. Probability Concepts in Engineering-Emphasis on Applications to Civil and Environmental Engineering. John Wiley & Sons, New York, USA, 2007.
- [48] Collins KR, Wen YK, Foutch DA. Dual-level seismic design: a reliability-based methodology. *Earthquake Engineering and Structural Dynamics* 1996; **25**(12):1433-1467.
- [49] Tubaldi E, Barbato M, Ghazizadeh S. A probabilistic performance-based risk assessment approach for seismic pounding with efficient application to linear systems. *Structural Safety* 2012; **36**:14-22.
- [50] European Committee for Standardization. *EN 15129:2010-Anti-seismic devices* Brussels, 2010.

NOTATION

D	Generic demand parameter	t	Time
DLS	Damage limitation state	u	Displacement relative to the ground
GM	Sample geometric mean	u_g	Ground motion
P_D	Probability of exceedance conditional on a_0	Π	Non-dimensional Π term
P_{D,T_L}	Risk of demand exceedance during T_L	α	Velocity exponent of the added viscous damper
S_A	Pseudo-spectral acceleration	β	Sample lognormal standard deviation (dispersion)
S_d	Spectral displacement	η	Normalized peak response parameter
T	Fundamental vibration period of the structure	λ	Dimensionless ground acceleration
T_L	Design life-time	λ_α	Constant depending on the velocity exponent α
ULS	Ultimate limit state	μ_m	Lognormal sample mean
a	Absolute acceleration	ν	Mean annual frequency of exceedance
c_L	Inherent viscous damping constant	ξ	Damping ratio inherent to the structural system
c_N	Damping constant of the added viscous damper	ξ_d	Added viscous damper damping ratio
f_d	Viscous damper force	τ	Dimensionless time instant
k	Stiffness of the structural system	ψ	Dimensionless displacement
m	Mass of the structural system	ω_0	Undamped circular frequency of the structure